14th Australasian Fluid Mechanics Conference
Adelaide University, Adelaide, Australia
10-14 December 2001

Further Evidence for a Transition in Small-Scale Turbulence

B. R. Pearson[1] and P. -Å. Krogstad[2]

[1]School of Mechanical, Materials, Manufacturing Engineering & Management.
University of Nottingham, Nottingham NG7 2RD, UK

[2]Dept. of Appl. Mech., Thermo. & Fluid Dynamics,
Norwegian University of Science & Technology, N-7491 Trondheim, NORWAY

Abstract

Measurements of the streamwise component u, on the centreline of a wake, confirm a transitional behaviour for normalized high-order moments of $\partial u/\partial x$, within the Taylor micro-scale Reynolds number R_λ range $600 \lesssim R_\lambda \lesssim 900$. This R_λ range is equivalent to the large-scale Reynolds number Re range of $1.3 \times 10^4 \lesssim Re \lesssim 2.8 \times 10^4$. The transition is short lived, with respect to the dissipation length scale η, and is not observed for velocity differences δu measured over differences greater than 10η. We suggest that these results are equivalent to previous observations known as "mixing" transitions $-$ transitions that are associated with the development of a truly 3-dimensional small-scale turbulent structure $-$ which are most probably a universal feature of turbulent shear flows.

Introduction

In view of the mounting experimental evidence for the intermittent nature of the energy dissipation rate, Kolmogorov[1] (hereafter K62) refined his earlier similarity hypotheses[2] (hereafter K41) for the description of the small-scale structure of turbulence at high Taylor micro-scale Reynolds number R_λ [$\equiv \langle u^2\rangle^{1/2}\lambda/\nu$, where λ is the Taylor micro-scale $= \langle u^2\rangle^{1/2}/\langle(\partial u/\partial x)^2\rangle^{1/2}$, x is the streamwise direction, u is the streamwise velocity fluctuation and ν is the kinematic viscosity, see Ref.[3] and references therein for a comprehensive historical review]. It is well accepted that small-scale intermittency is attributable to intense small-scale vortical structures[3]. Experimental evidence for the effect of these structures are the "wide" exponential tails of the velocity derivative probability density functions (pdf). A consequence of exponential tales for the velocity derivative pdfs are moment-order magnitudes higher than the corresponding Gaussian value. Also, the pdf tails are known to extend as R_λ increases. An analytical consequence of Kolmogorov's K62 refinement is that the moments of velocity derivative pdfs are R_λ dependent. Data assembled for the skewness and flatness factors of $\partial u/\partial x$ over the large R_λ range $2 \lesssim R_\lambda \lesssim 30000$ shows qualitative agreement with this expectation[3]. To provide such a large R_λ spread, data have been assembled from many different types of turbulent flows and direct numerical simulations (DNS) $-$ though individual experiments contributed a limited R_λ range of results. The firmly held view is that such collections, as shown in Ref.[3], provide unequivocal evidence for the increasing effects of small-scale intermittency with R_λ.

There have been few concentrated efforts to generate turbulence, over a reasonable R_λ range in the same experimental set-up. One instance is turbulence generated in a confined, rotating, shear-flow[4]. Importantly, R_λ is raised by very small increments over the significant range of $150 - 5040$. A transitional behaviour for high-order moments of $\partial u/\partial x$ with R_λ is observed. For example, the flatness factor, $F_{\partial u/\partial x}[\equiv \langle(\partial u/\partial x)^4\rangle/\langle(\partial u/\partial x)^2\rangle^2]$, increases up until $R_\lambda \approx 600$, in agreement with the results[3], but then decreases for the range $600 \lesssim R_\lambda \lesssim 900$, after which it increases again with R_λ. These results are $-$ for the most part $-$ criticized for their unconventional flow geometry and instrumentation[3]. The aim of this work is to document the R_λ dependency for high-order moments of $\partial u/\partial x$ $-$ in particular $F_{\partial u/\partial x}$ $-$ in a given flow over a reasonable range of R_λ. To avoid potential criticism, measurements are made, using a conventional wind-tunnel, in the turbulent wake behind a porous body. A well-proven constant temperature anemometer (CTA) design, combined with a single-wire probe of adequate resolution, is used.

Experimental Details

The measurements are made in a *NORMAN* grid. The geometry is composed of a perforated plate superimposed over a bi-plane grid of square rods. Further details of the geometry and the resulting flow are described elsewhere[5] and only a brief description of the experimental set-up is given here. The grid is located in a recirculating wind-tunnel with a test section of 2.7×1.8 m^2 cross section and length 11 m. The central three rows of the original bi-plane grid (mesh size $M = 240$ mm, original solidity $\sigma = 28\%$) have alternate meshes blocked (final $\sigma = 42\%$). Signals of u on the wake centreline at $x/M = 40$, are acquired with a CTA[6] combined with a single hot-wire probe made of 1.27μm diameter Wollaston (Pt-10%Rh) wire. The mean velocity, at the measurement station, ranges from $2.3 - 14.1$ m/s and the ratio $\langle u^2\rangle^{1/2}/U$ is a constant value of 0.17. The wire overheat ratio is 1.65 and the instantaneous bridge voltage is buck-and-gained and the amplified signal is low-pass filtered f_{lp} with the sampling frequency f_s always at least twice f_{lp}. To avoid electronic noise contamination, f_{lp} is set immediately prior to which electronic noise is noticed to unduly infiltrate the dissipation spectrum $-$ assumed to be represented by $k_1^2\phi_u(k_1)$ [here, k_1 is the 1-dimensional longitudinal wavenumber $k_1 \equiv 2\pi f/U$ and $\phi_u(k_1)$ the 1-dimensional energy spectrum of u such that $\langle u^2\rangle = \int_0^\infty \phi_u(k_1)dk_1$]. This is possible because the low-pass filter, *Frequency Devices Model 900*, has a frequency resolution of 1 : 499 per decade. The voltage signal is recorded with 12$-$bit resolution. Due to the non-linearity of the probe velocity-voltage calibration, converted velocity data needed to be saved with 13-bit resolution to avoid a loss of resolution at low velocities. Time differences τ and frequencies f are converted to streamwise distance r ($\equiv \tau U$) and k_1 respectively using Taylor's hypothesis. The mean energy dissipation rate $\langle\varepsilon\rangle$ is estimated, assuming isotropy amongst the velocity derivative components, as $\langle\varepsilon\rangle \equiv \varepsilon_{iso} = 15\nu\int_0^\infty k_1^2\phi_u(k_1)dk_1$. The largest dissipation length scale $\eta \equiv (\nu^3/\varepsilon_{iso})^{1/4}$ is $0.48m$m and the smallest is $0.12m$m and the non-dimensional wire sensing length range is $0.48 - 1.8$. Record lengths range from ≈ 7200s for the lowest mean velocity to ≈ 1500s for the highest. In the analysis to follow, a large length scale l, indicative of the most energetic eddies, will be required. We estimate l from the inverse wavenumber $1/k_{1,max}$ where $k_1\phi_u(k_1)$ is a maximum. Further details and justification can be found in Ref. [11].

As R_λ increases, the wire resolution decreases. All wires used in this investigation have more than adequate frequency response − a built-in square-wave impulse (300Hz) applied to the anemometer bridge typically gives more than 25kHz compared to a maximum dissipation frequency $f_\kappa \equiv U/2\pi\eta$ of 18.5kHz. The CTA bridge is based on a well-proven design[6]. The novelty of this design is the omission of cable-inductance compensation often found in commercial anemometer bridges. An obvious consequence of the in-house design is that fine-scale measurements are extremely dependent on wire resolution and response, whereas commercial anemometers are known to automatically apply an inductance compensation of $\approx +6dB$ per octave for $f > 1000$Hz. With our anemometers, an adequate measurement is only possible with a probe of adequate frequency response and resolution, whereas with commercial anemometers, the added cable-inductance compensation may give a false sense of security for a fine-scale measurement when used with a probe of inadequate resolution. It is worth noting that the majority of the experimental results presented in Ref.[3] were obtained with commercial anemometers.

Results

The R_λ dependence of $F_{\partial u/\partial x}$

Given a decreasing wire resolution, it is more convincing to compare results, over the resulting R_λ range $430 \lesssim R_\lambda \lesssim 1150$, at the same spatial resolution. This is accomplished with the use of normalized $4th$-order structure functions of the longitudinal velocity increment $\delta u(r^*) = u(x^* + r^*) - u(x^*)$ [here, r is the spatial separation between instances of u and * denotes normalization by η],

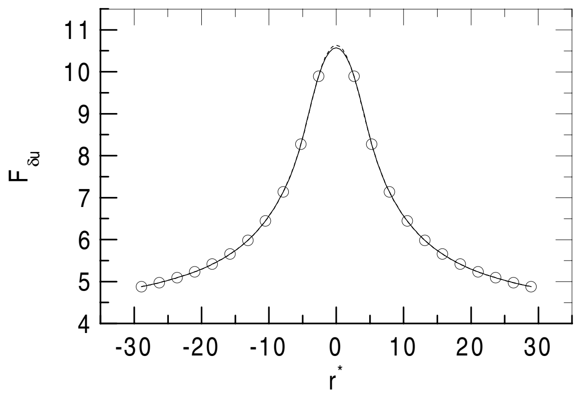

Figure 1: An example of using cubic splines to estimate $F_{\delta u}$, $R_\lambda \approx 900$. ◯, experimental data; ———, with no weighting; − − −   , with log weighting.

$$F_{\delta u} = \langle[\delta u(r^*)]^4\rangle / \langle[\delta u(r^*)]^2\rangle^2 \qquad . \tag{1}$$

The approach allows the examination of the R_λ dependence of $F_{\delta u}$ for decreasing values of r^*. To estimate $F_{\partial u/\partial x}$, i.e. $F_{\delta u(r^* \to 0)}$, homogeneity of the smallest scales is assumed for $\delta u(r^*)$. Cubic splines are fitted to the resulting distribution of $F_{\delta u}$ over the range of $-30 < r^* < 30$. The exercise is repeated with a logarithmic weighting to $F_{\delta u}$. Figure 1 shows an example of the resulting distributions of $F_{\delta u}$ at $R_\lambda \approx 900$. There is little difference between weighted and non-weighted results. The behavior of $F_{\delta u}$ is investigated at values of $r^* = 0$, 2, 4 and 10. Figure 2 shows the resulting $F_{\delta u}$ distributions versus R_λ for the chosen values of r^*. A transitional behaviour for $F_{\delta u}$ is observed within the range $600 \lesssim R_\lambda \lesssim 900$. At $r^* = 2$, which is the limit of the probe resolution, the magnitude of $F_{\delta u}$ agrees with, and

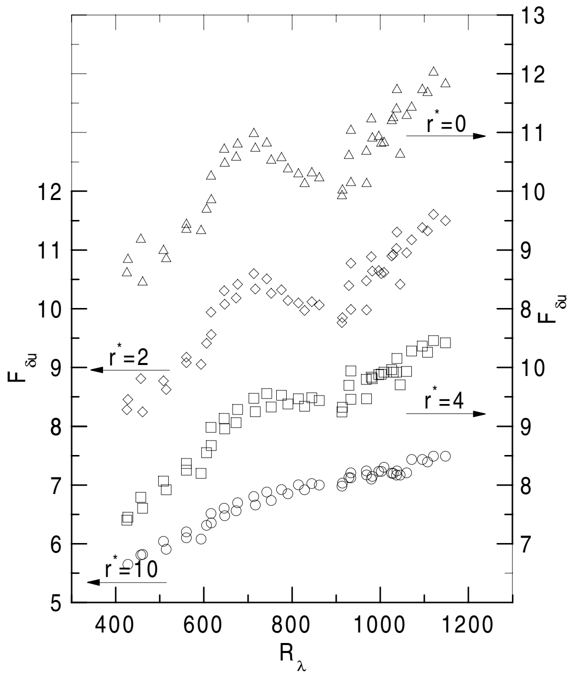

Figure 2: The R_λ dependence of $F_{\delta u}$ in a *NORMAN* grid flow, $430 < R_\lambda < 1150$. △, $r^* = 0$; ◇, $r^* = 2$; □, $r^* = 4$; ◯, $r^* = 10$

occurs over the same range of R_λ as Ref.[4]. Figure 2 shows that the transition in $F_{\delta u}$ is dependent on r^* up until $r^* \approx 10$. This suggests that the phenomenon responsible for the transition may have a characteristic length scale $\approx 20\eta$. It is interesting to recall that the diameter range for the intense small-scale vortical structures called "worms" has been shown to be $\lesssim 16\eta$[8].

Checks on the Inertial- and Large-Scale Behaviour

A potential criticism for our work is that the small-scale transition is due to unwanted anomalous large-scale behaviour. In this subsection we will carry out some simple checks. Prior to this, we have checked that $\langle u^2\rangle^{1/2}/U$ and L do not change appreciably with R_λ - certainly not $\sim O(10\%)$ as seen for the change in $F_{\partial u/\partial x}$. Within the framework of K41 the expectation for $\langle(\delta u^*)^n\rangle$ is

$$\langle(\delta u^*)^n\rangle \sim C_n r^{*n/3} \qquad , \tag{2}$$

with C_n universal. However, for modern refined similarity hypotheses, for example K62, small-scale intermittency is held responsible for the modification to the power-law exponent for r^*, such that,

$$\langle(\delta u^*)^n\rangle \sim C'_n r^{*\zeta(n)} \qquad , \tag{3}$$

with C'_n no longer universal (in the sense of being R_λ independent). Figure 3 shows $\langle(\delta u^*)^2\rangle$ and $\langle(\delta u^*)^4\rangle$ normalized by dissipation scales. There are three main ranges of interest: the dissipative range $r^* \leqslant 60$, the inertial range $60 \leqslant r^* \leqslant L^*$ and the large-scale or de-correlated range, $r^* \gg L^*$. Within experimental uncertainty, there is no R_λ dependence for $\langle(\delta u^*)^2\rangle$ in either the dissipative or inertial ranges − specifically, for the inertial range, there is no R_λ dependence for either $C'(2)$ or $\zeta(2)$. For $\langle(\delta u^*)^4\rangle$, there is R_λ dependence in magnitude throughout the dissipative range and for $C'(4)$ through the inertial range. Although, inertial range scalings Eq.(3) have been discussed elsewhere[5], the inertial range scalings are R_λ independent with $\zeta(2) \simeq 0.73$ and $\zeta(4) \simeq 1.34$ for the range $60 \leqslant r^* \leqslant 500$. As L^* is approached, the $\langle(\delta u^*)^2\rangle$ and $\langle(\delta u^*)^4\rangle$ distributions begin to peel-off; with the r^* at which this begins increasing with

R_λ. The magnitude of the de-correlated region is R_λ dependent and obeys (not shown, see Ref. [9]) $\langle(\delta u^*)^2\rangle = 2R_\lambda/\sqrt{15}$ and $\langle(\delta u^*)^4\rangle = 2\,(F_u+3)\,R_\lambda^2/15$ where $F_u = \langle u^4\rangle/\langle u^2\rangle^2$. With

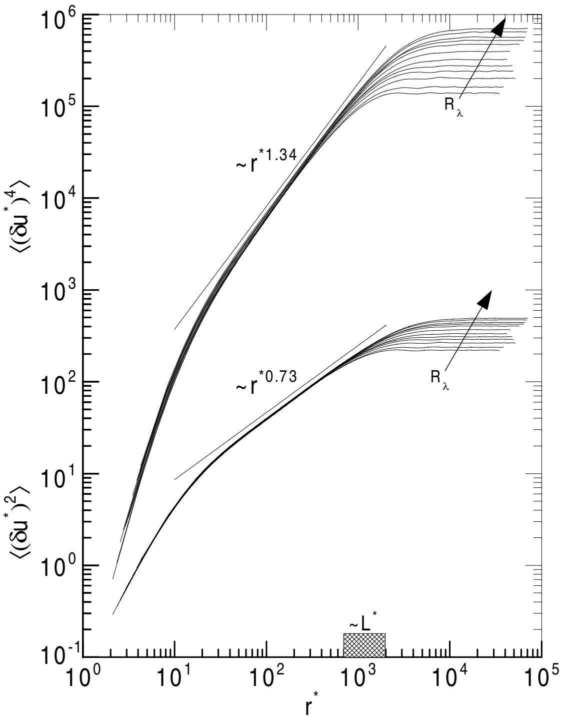

Figure 3: The R_λ dependence of $\langle(\delta u^*)^2\rangle$ and $\langle(\delta u^*)^4\rangle$ in a *NORMAN* grid flow, $430 < R_\lambda < 1150$.

$\zeta(2) \simeq 0.73$ and $\zeta(4) \simeq 1.34$, we can expect $F_{\delta u}$ to behave like $r^{*\zeta(4)-2\zeta(2)} = r^{*-0.12}$. Figure 4 shows this to be the case. We do not consider the difference between -0.10 and -0.12 to be experimentally significant and we concur that $F_{\delta u} = r^{*-0.10}$, independent of R_λ[3]. Figure 4 delimits two R_λ examples as the upper and lower bounds for which the transition in $F_{\partial u/\partial x}$ occurs. There is no untoward behaviour in the inertial- or large-scale ranges and both distributions follow that of their immediate neighbor. For a Gaussian process, the flatness factor $F = 3$. Figure 4 shows that such a magnitude for $F_{\delta u}$ is only approximately approached as $r^* \to \infty$ [strictly $F_{\delta u, r^*\to\infty} = (F_u+3)/2$]. The R_λ dependence for the magnitude in $F_{\delta u}$, shown in Figure 4, is attributable to the R_λ dependence for $C'(4)$ shown in Figure 3. In summary, Figures 3 and 4 show that there is nothing untoward about the R_λ behaviour of the inertial- and large-scale regions for the distributions of $\langle(\delta u^*)^2\rangle$ and $\langle(\delta u^*)^4\rangle$. We can safely rule out any "transitional" behaviour for inertial- or large-scales being responsible for the retrograde behaviour we have observed, in Figure 2, for $F_{\partial u/\partial x}$.

Further Evidence for a Transition of Small-Scales

In a recent paper, Dimotakis[10] reviews the available evidence for what he calls the "mixing transition". He shows, for many free shear flows, that a transition, visualized as a dramatic increase in "dimpling" of the large-scale structures, takes place within the large-scale Reynolds number $Re\left[\equiv \left\langle u^2\right\rangle^{1/2} L/\nu\right]$ range $10^4 \lesssim Re \lesssim 2\times10^4$. The Re range appears to be universal. The transition is suggested to be the signature of the establishment of a truly 3-dimensional small-scale structure − a necessary requirement for fully developed turbulent flows. However, he does not dismiss the possibility that manifestations of the transition could be slightly flow dependent − citing that the mechanism responsible for the creation of the small-scale 3-dimensional structure is flow dependent.

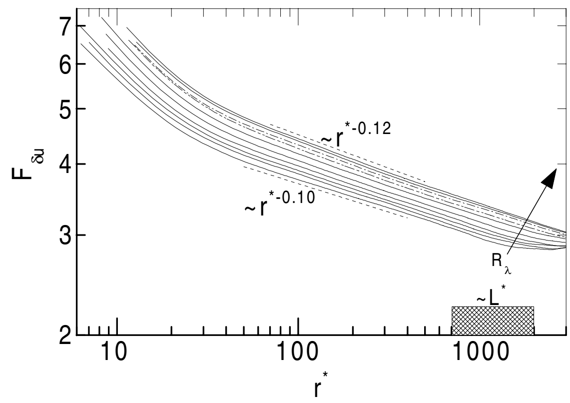

Figure 4: The R_λ dependence for $F_{\delta u}$ in a *NORMAN* grid flow, $430 < R_\lambda < 1150$. — — — , a guide only; — - - —, $R_\lambda \approx 820$; — - —, $R_\lambda \approx 915$;

The explanation[10] for the "mixing" transition requires the introduction of a new inner length scale l called the *laminar-layer thickness*. The scale l is generated by viscosity after a sweep of size L across the transverse turbulent layer. The place of l, in the usual hierarchy of turbulent scales, is $\eta \ll r \ll l \ll L$. It is proposed that not until the smaller scales r are de-coupled from this new scale l can a turbulent flow be considered fully developed. Scaling arguments, offered in Ref.[10], suggest that this will not occur until $10^4 \lesssim Re \lesssim 2\times10^4$ − a Re range suggested to be equivalent to $100 \lesssim R_\lambda \lesssim 140$ i.e. $R_\lambda = \sqrt{Re}$. However, we believe that Dimotakis' estimate of R_λ from Re should be, more justifiably, estimated as

$$R_\lambda = \sqrt{15Re/C_\varepsilon} \quad . \tag{4}$$

The factor C_ε is the non-dimensionalised energy dissipation rate which is expected to be independent of viscosity i.e. R_λ independent. For measurements limited to one velocity component, a common form of non-dimensionalization of $\langle\varepsilon\rangle$ is,

$$C_\varepsilon = \varepsilon_{iso} L \Big/ \left\langle u^2\right\rangle^{3/2} \quad . \tag{5}$$

Figure 5 shows sufficient evidence to accept that C_ε is R_λ independent for $R_\lambda > 300$ and $C_\varepsilon \approx 0.5$ appears to be a reasonable universal estimate for shear flows free of *strong* mean shear. The result is, seemingly, more specific than the view that the magnitude of C_ε is flow dependent[12] and of $O(1)$ and we believe such a view needs modification, especially with respect to the method of estimating L and the value of R_λ. These issues are discussed in detail in Ref. [11]. Figure 5 suggests that there is insufficient separation between the energy and dissipation scales, for shear flows in the range $100 \lesssim R_\lambda \lesssim 140$, which is necessary requirement for C_ε to obtain constancy. However, Figure 5 does suggest that the rate of approach of C_ε to R_λ independence appears to be flow dependent. Using $C_\varepsilon = 0.5$, Dimotakis' range for the transition appears more likely to be $550 \lesssim R_\lambda \lesssim 775$. The agreement between this "new" R_λ range and the transition range for $F_{\partial u/\partial x}$ shown in our work here, Figure 2, and that of Ref.[4] may not be so coincidental. Indeed, Ref.[8] demonstrates that the transitional behaviour for $F_{\partial u/\partial x}$ is most likely attributable to a "change" in the small-scale structure of turbulence. It is not implausible that this "change" is the establishment of a truly 3-dimensional small-scale structure.

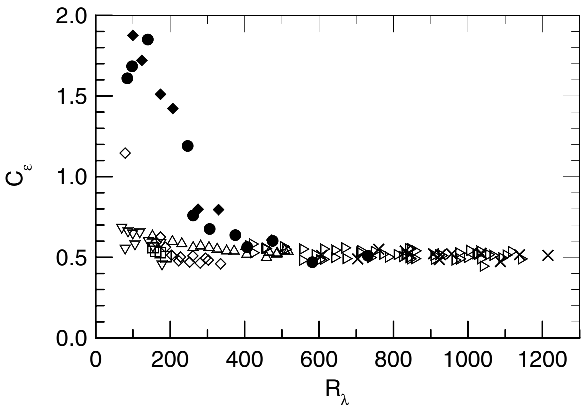

Figure 5: Normalized dissipation rate, $C_\varepsilon \equiv \varepsilon_{iso} L / \langle u^2 \rangle^{3/2}$ [Eq. (5)] for a number of shear flows. Details as found in this work and Refs.[7, 11]. $\square$, circular disk, $154 \lesssim R_\lambda \lesssim 188$; ∇, pipe, $70 \lesssim R_\lambda \lesssim 178$; $\diamond$, normal plate, $79 \lesssim R_\lambda \lesssim 335$; $\triangle$, *NORMAN* grid , $174 \lesssim R_\lambda \lesssim 516$; $\times$, *NORMAN* grid (slight mean shear, $dU/dy \approx dU/dy|_{max}/2$), $607 \lesssim R_\lambda \lesssim 1217$;$\triangleright$, *NORMAN* grid (zero mean shear), $425 \lesssim R_\lambda \lesssim 1120$; $\bullet$, "active" grid, (Refs. [13, 14]) $100 \lesssim R_\lambda \lesssim 731$;$\blacklozenge$, "active" grid, (Ref. [13]) with L_u estimated by Ref. [15]. For Ref. [13] data we estimate $L_p \approx 0.1$ m and for Ref. [14] data we estimate $L_p \approx 0.225$ m[14].

Final Remarks & Conclusions

We have observed transitional behaviors for high-order small-scale quantities e.g. $F_{\partial u/\partial x}$. We believe our observations are reconcilable with the visual observations of Dimotakis[10] if relation (4), that between R_λ and Re, is adopted. Such transitions are probably a signature for the development of a truly 3-dimensional small-scale structure $-$ a necessary ingredient for fully developed turbulence. Flows with R_λ below this range are less likely to be universal.

Acknowledgments

We gratefully acknowledge the assistance of the technical staff at NTNU. BRP acknowledges helpful conversations with P. Tabeling and J.C. Vassilicos.

References

[1] Kolmogorov, A. N., 1962, A Refinement of Previous Hypotheses Concerning the Local Structure of Turbulence in a Viscous Incompressible Fluid at High Reynolds Number, *J. Fluid Mech.* **13**, 82-85.

[2] Kolmogorov, A. N., 1941, The Local Structure of Turbulence in an Incompressible Fluid for Very Large Reynolds Numbers, *Dokl. Akad. Nauk. SSSR* **30**, 299-303.

[3] Sreenivasan, K. R. & Antonia, R. A., 1997, The Phenomenology of Small-Scale Turbulence, *Ann. Rev. Fluid Mech.* **29**, 435-472.

[4] Tabeling, P., Zocchi, G., Belin, F., Maurer, J. & Willaime, H., 1996, Probability Density Functions, Skewness, and Flatness in Large Reynolds Number Turbulence, *Phys. Rev. E* **53**, 1613-1621.

[5] Pearson, B. R., Krogstad, P. -Å. & van de Water, W., 2000, The Effect of Large-Scale Forcing on the Small-Scale Structure of Turbulence, submitted to *Phys. Rev. E.*

[6] Miller, I. S., Shah, D. A. & Antonia, R. A., 1987, A Constant Temperature Hot-Wire Anemometer, *J. Phys. E: Sci. Instrum.* **20**, 311-314.

[7] Pearson, B. R., Krogstad, P. -Å. & Carper, M. A., 2001, Re Dependence of the Energy Dissipation Rate and Spectrum in Shear Flows, In *Proceedings of the 14th Australasian Fluid Mechanics Conference,* Adelaide.

[8] Belin, F., Maurer, J., Tabeling, P., & Willaime, H., 1997, Velocity gradient distributions in fully developed turbulence: an experimental study, *Phys. Fluids* **9**, 3843-3850.

[9] Pearson, B. R. & Antonia, R. A., 2001, Reynolds Number Dependence of Turbulent Velocity and Pressure Increments, *J. Fluid Mech.* **444**, 343-382.

[10] Dimotakis, P. E, 2000, The Mixing Transition in Turbulent Flows, *J. Fluid Mech.* **409**, 69-98.

[11] Pearson, B. R., Krogstad, P. -Å. & van de Water, W., 2001, Measurement of the Energy Dissipation Rate in Shear Flows, to appear *Phys. Fluids*.

[12] Sreenivasan, K. R., 1995, "The Energy Dissipation Rate in Turbulent Shear Flows," in *Developments in Fluid Dynamics and Aerospace Engineering*, (Eds. S. M. Deshpande, A. Prabhu, K. R. Sreenivasan, & P. R. Viswanath) Interline, Bangalore, India, pp.159.

[13] Mydlarski, L. & Warhaft, Z., 1996, "On the Onset of High-Reynolds Number Grid-Generated Wind Tunnel Turbulence," *J. Fluid Mech.* **320,** 331-368.

[14] Mydlarski, L. & Warhaft, Z., 1998,"Passive scalar statistics in high-Péclet-number grid turbulence," *J. Fluid Mech.* **358**, 135-175.

[15] Gamard, S. & George, W. K., 1999, "Reynolds Number Dependence of Energy Spectra in the Overlap Region of Isotropic Turbulence," *Flow,Turb. and Comb.* **63,** 443-477.